SURFACE TOPOGRAPHY OF A PALLADIUM CATHODE AFTER ELECTROLYSIS IN HEAVY WATER

ELECTROLYTIC DEVICES

TECHNICAL NOTE

KEYWORDS: *palladium, electrolysis, topography*

DAVID S. SILVER *Phillips Laboratory, Edwards Air Force Base, California*

JOHN DASH and PATRICK S. KEEFE *Portland State University*
Physics Department, P.O. Box 751, Portland, Oregon 97207

Received March 2, 1992
Accepted for Publication June 18, 1993

Electrolysis was performed with a palladium cathode and an electrolyte containing both hydrogen and deuterium ions. The cathode bends toward the anode during this process. Examination of both the concave and the convex surfaces with the scanning electron microscope, scanning tunneling microscope, and atomic force microscope shows unusual surface characteristics. Rimmed craters with faceted crystals inside and multitextured surfaces were observed on an electrolyzed palladium cathode but not on palladium that had not been electrolyzed.

INTRODUCTION

The phenomena that occur during the electrolysis of heavy water with a palladium cathode have been studied extensively since the reports of the possibility of nuclear fusion in this process.[1,2] It has been suggested that nuclear fusion may occur in this system by the combination of hydrogen and deuterium rather than deuterium and deuterium and that the energy released may be absorbed by the palladium lattice.[3]

In the study reported here, a large amount of hydrogen is produced at the cathode along with deuterium. Microscopic features produced on the palladium surface have been characterized by using the scanning electron microscope (SEM), scanning tunneling microscope (STM), and atomic force microscope (AFM).

EXPERIMENTAL METHODS AND RESULTS

The electrolyte used in this experiment contained 20 ml D_2O and 3.5 ml H_2SO_4. Palladium foil ~25 μm thick was produced by cold rolling palladium from a rod to an ~90% reduction in thickness. The palladium foil was scratched on the surface, and the area of the scratch was photographed (Fig. 1a). The foil was then immersed in the electrolyte for 1 h at 27°C. The same area was then photographed (Fig. 1b). Because there was no observable change on the surface and no weight change, it was concluded that the palladium foil was chemically inert in the electrolyte.

The palladium cathode used for electrolysis was made by cold rolling a high-purity single crystal from ~250- to 25-μm thickness. Platinum foil was used for the anode. Electrolysis was performed at room temperature, using a 50-ml beaker to contain the electrodes and electrolyte. A constant current of 0.5 A and a cathode current density of ~0.25 A/cm^2 were passed for 12 min. The cell voltage was ~3.5 V. The palladium cathode rapidly distorted during electrolysis, bending toward the platinum anode. After electrolysis, this was examined with an SEM. Surface damage such as that shown in Fig. 2a was observed on the convex surface of the palladium cathode.

In addition to the large pit with needles inside, there were smaller pits randomly scattered over the surface. The electrolyte temperature rose to 29°C during electrolysis, but there was no control cell in series for comparative temperature measurements. An energy-dispersive spectroscopy spectrum of the surface showed that only palladium was present.

Figure 2b is a view of the concave surface of the cathode, which faced the anode during electrolysis. The magnification is the same as in Fig. 2a. Lines from the cold-rolling process that are prominent in Fig. 2a are not evident in Fig. 2b. Instead, curved lines, such as that indicated by the arrow, suggest that surface relief effects were produced during electrolysis. The pit has three straight sides, suggesting that it occurred along definite crystal planes during electrolysis. If the pit had occurred during cold rolling, it would be elongated in the rolling direction.

Small surface pits, such as that indicated by the arrow on Fig. 2a, were examined with the STM and with the AFM. As a control, a piece of cold-rolled single-crystal foil not used in electrolysis was also examined in the STM and AFM.

The AFM observations were accomplished in air at normal room temperatures with a Nanoscope II microscope. Observations were generally made by using two different image modes: the force mode, which means that vertical dimensions are captured in the nanonewton scale, and the height mode, which means that vertical dimensions are captured in the nanometre scale. The latter mode represents the surface height. Height-mode images appear less sharp than their force-mode counterparts but yield accurate height definition. Although force-mode images lose information about height, they yield surface detail.

The tip is ideally one or a few atoms wide at one end and is attached at the other end to a cantilever that deflects as the

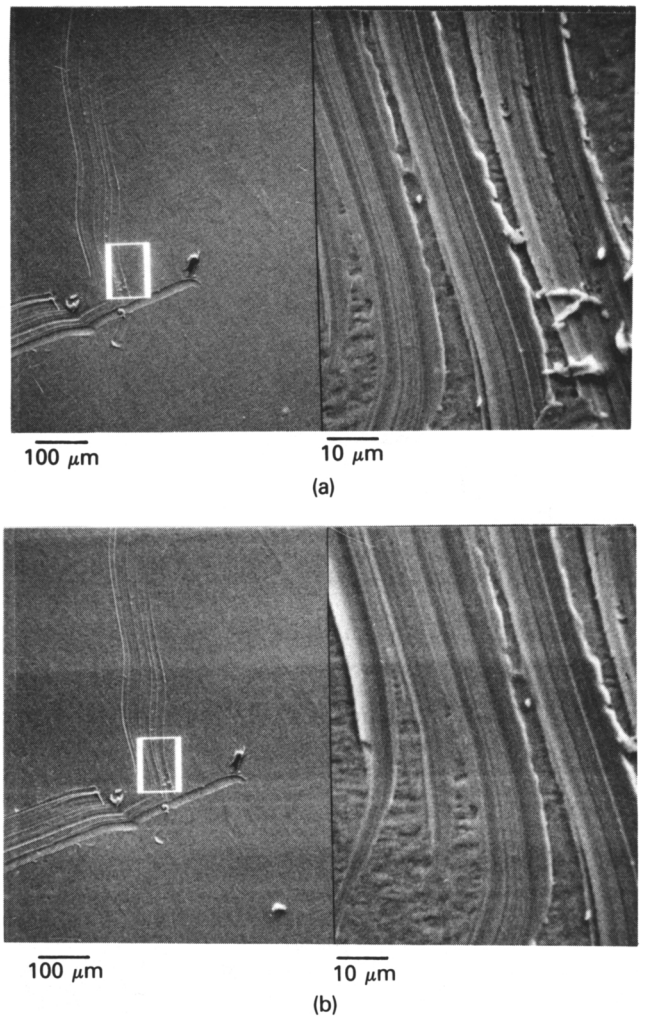

Fig. 1. SEM micrographs of the same area of the palladium cathode (a) before and (b) after immersion in the electrolyte for 1 h to determine whether the chemicals in the electrolyte had any reaction with palladium. There was no weight change, and it appears that there was no chemical reaction.

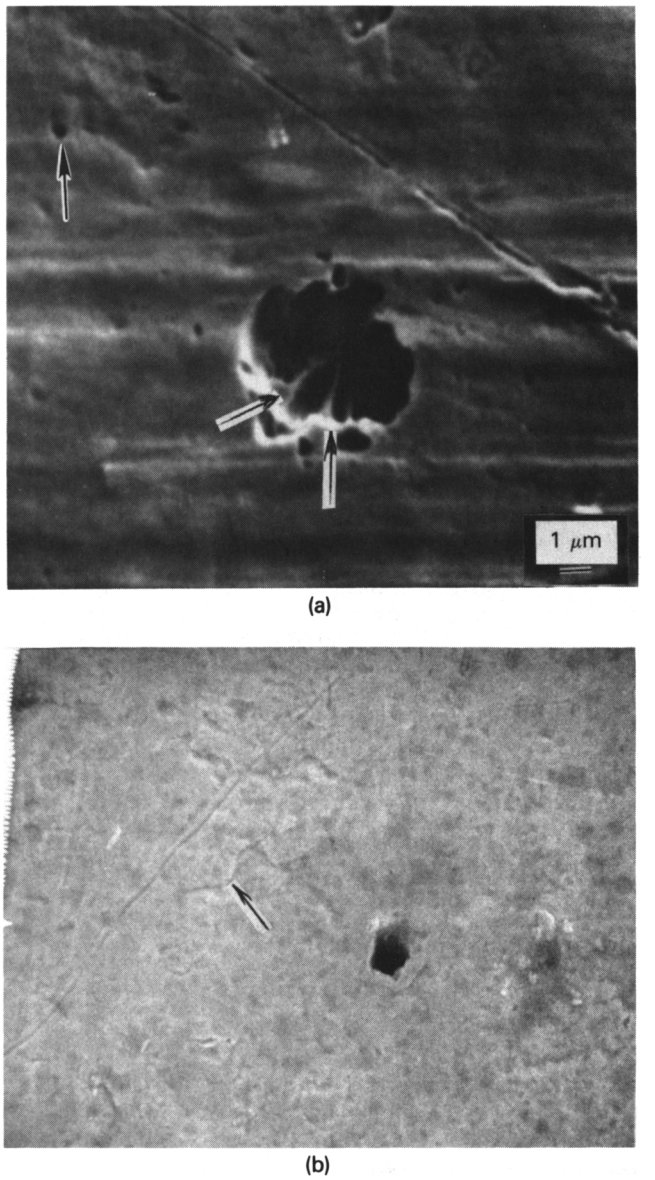

Fig. 2. (a) SEM photo of a palladium cathode on the side facing away from the anode (convex) after electrolysis for 12 min. The large pit is thought to have occurred during electrolysis. The horizontal lines were caused by the cold-rolling process that preceded electrolysis. Note that the large pit is not extended in the direction of the horizontal lines. This minimizes the possibility that the pit was present before electrolysis. Pits such as that indicated by the upper left arrow were examined with the STM and AFM. The arrows in the lower portion of the photograph indicate features similar to needles that extend into the pit. (b) SEM photo of the same palladium cathode, but on the opposite, concave side, which faced the anode. Same magnification as (a). Lines from cold rolling are not evident. The pit and the curved line suggest changes that occurred during electrolysis.

tip scans the sample. This deflection is monitored by a feedback system and recorded, eventually to be translated into an image on a monitor. The height mode requires that the height of the sample beneath the tip be adjusted, as the cantilever deflections remain constant during the scanning process. The force mode, however, requires that the cantilever deflections be recorded while the height remains nearly constant during the scanning process.

Other forces tend to interact between sample and tip, such as electrostatic forces and surface tension. Acquiring AFM images for the palladium electrode was difficult and time-consuming because of these other forces. Hours of repeated attempts to produce an image of, say, a single surface crater, usually resulted in frustration because the roughness of the surface almost always tore the tip and cantilever apart. A full day might produce one or two images (including those taken at higher step magnifications over the same area) at most. The control sample, on the other hand, allowed far easier imaging because of its flatter morphology, and sets of images could be obtained almost at will.

Difficulty was also encountered in using the STM on the palladium electrode because of the rough nature of its surface. The STM operates similarly to the AFM but uses a tunneling current, a quantum-mechanical phenomenon, between its tip and the sample. This instrument is therefore confined

to scanning conducting surfaces only. The height mode was used for the STM in this research, which means that the z scale is in nanometres. As the tunneling current is kept constant, a feedback loop varies the height of the tip as it scans over the sample. A platinum-iridium tip was used, and again, observations were made in air at room temperatures with a Nanoscope II microscope.

The advantage of utilizing equipment such as the AFM and STM is that far greater resolution of surface structure can be achieved over, say, the SEM or an optical microscope. Resolution with the SEM is not sufficient to resolve fine details on the interior of the craters that form on the surface of the palladium electrode.

Figures 3a and 3b, respectively, show 10-μm-square images of the unexposed palladium surface and the convex side of the electrolyzed palladium cathode surface, captured in the force mode. Much more detail is apparent than in the Fig. 2 SEM images. The unexposed surface shows vertical lines, due to grinding marks on the steel rolls used for the cold rolling, while the electrolyzed cathode surface, seen at the same scale, exhibits a rough feature of ~6-μm diameter. Portions of this rough feature are enlarged in Figs. 3c and 3d to show clearly the angular facets and rounded nodules that comprise this feature. The facets are at an angle of ~73 deg, which suggests that these are traces of {111} planes and that the plane of the photograph is approximately {110}.

Additional information about the feature in Fig. 3b was obtained by using the AFM in the height mode. This is shown in Fig. 4, which depicts a mound above the surface with an irregular crater within it. The event that produced this feature has obliterated the features of the cold-rolled surface shown in Fig. 3a. It seems most probable that this event was caused by a violent internal reaction of the gases produced by electrolysis with the outer layers of the palladium cathode.

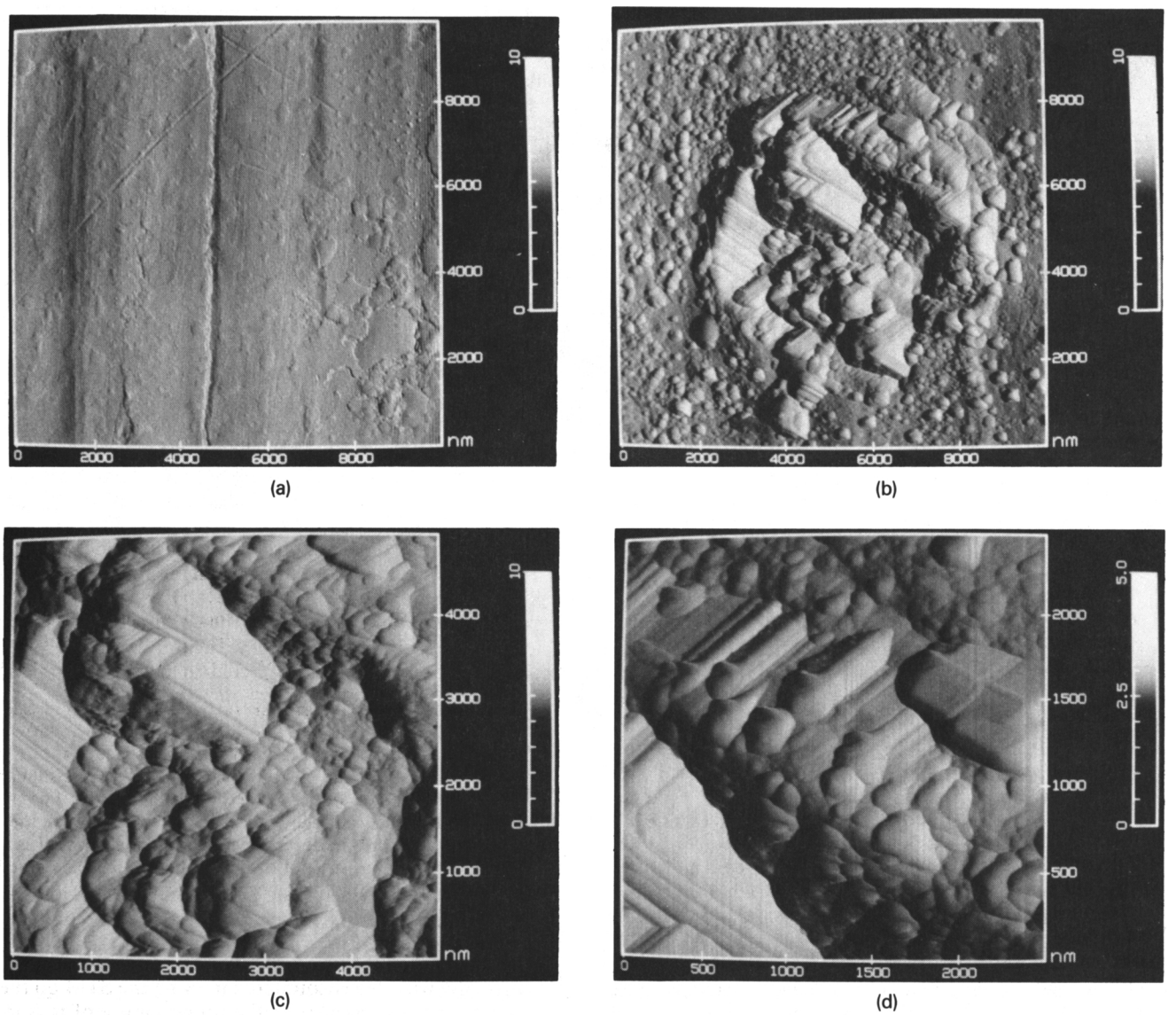

Fig. 3. AFM images of (a) palladium foil surface after cold rolling (the vertical lines resulted from contact with the steel rolls); (b) palladium cathode surface after electrolysis for 12 min; (c) and (d) enlargements of surface pit in (b) to show the rounded and faceted features.

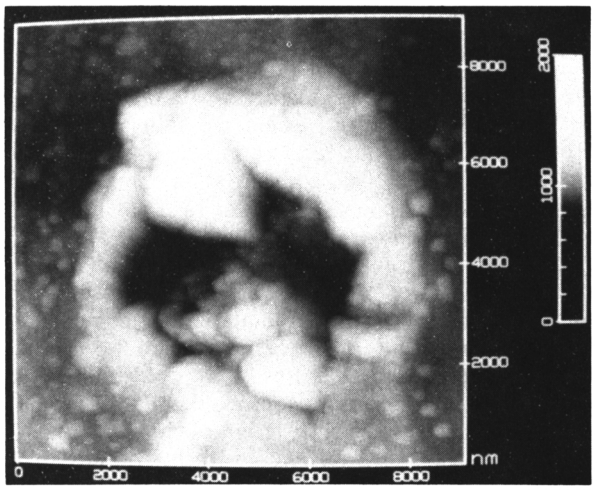

(a)

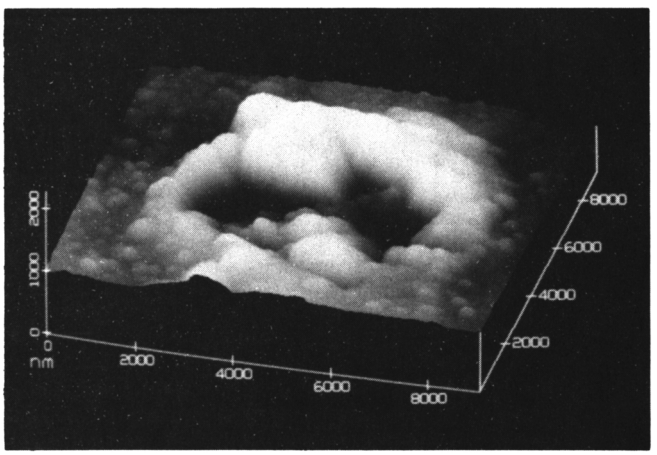

(b)

Fig. 4. Height-mode images of Fig. 3b, showing that this feature is a crater with a rim.

Chemical reaction is improbable because the chemical used does not react with palladium. Electrochemical dissolution is improbable at the palladium cathode. Electroplating is unlikely to produce a mound with a crater. It is well known that asperities that occur during electroplating tend to be dendritic.

If the foregoing reasoning is accepted, then the most probable event, an internal eruption of the metal near the surface, must have occurred at a temperature that produced rounded and faceted crystals unrelated to the cold-rolling process. It seems most probable that the features associated with this crater were caused by localized surface melting and subsequent crystallization.

Figures 5a, 5b, and 5c show another crater on the convex side of the electrode surface. Figure 5a illustrates in the height mode a bowl-shaped cavity that plunges beneath the rest of the surface, and Fig. 5b illustrates the same cavity in the force mode, showing its striations, which converge toward the center. The angle between the striations is ~66 deg, again suggesting that these may be {111} plane traces. Figure 5c is a line section of Fig. 5a, which places two arrows on the line that represents a contour of the crater. The two arrows indicate a vertical distance and a horizontal distance between them, the former reading >280 nm for the crater. The total diameter of the well is ~1.8 μm.

Generally, STM images of the cold-rolled palladium sample and the electrolyzed palladium cathode yielded those seen in Figs. 6a and 6b, respectively. These images are rotated 30 deg about the x axis for viewing appreciation. Once again, the vertical scales, seen on the left side of each image, are identical: 400 nm in height for the height-mode variation. Once again, light intensity and contrast are kept the same for each image for comparison. With scans made on 4-μm squares, the electrolyzed cathode clearly possesses the more detailed surface of the two. Surface roughness on the cathode appears to be greatly enhanced over that on the cold-rolled sample. Others who claim to have seen this effect when using the STM believe that hydrogen ions are actually absorbed and reduced on the surface. Some of these permeate into the palladium structure, producing porosity.[4] These ions accumulate into the regions separated by lattice defects and cause them to swell. These swollen regions along with craters, were typically observed with the STM.

Figure 7a presents another STM image of the electrolyzed palladium cathode, here shown for a 1- × 1-μm scan. A single nodule appears to be made up of smaller nodules. Figure 7b shows a pit with a gradual decline, ~200 nm wide and >35 nm deep, which is typically encountered on this surface.

Figure 8a is a typical AFM height-mode image of the cold-rolled palladium surface, and Fig. 8b is an AFM height-mode image of a region on the concave side of the palladium cathode, which faced the anode during electrolysis. The z scale, identical for both, reveals that the cold-rolled surface again appears flat, while the electrode shows an enormous unevenness, in this case, a pit so deep that the AFM had difficulty reaching the bottom. The latter is indicated by Fig. 8c, a contour of Fig. 8b. The pit drops off >1.6 μm from its edge. There also appears to be more than one surface level. The flat line to the right indicates that this part of the surface rises higher than the scaling allows, meaning that the surface area on the left of the pit and that on the right are at two different elevations. This area did not allow a force-mode capture. Figure 8d is another common rough surface area seen in the same mode on the same side of the cathode, yielding 2- to 3-μm-diam mountain-like structures that rise >1 μm high above the plane surface. These configurations, which were never seen on either side of the cold-rolled palladium chip, made imaging with the AFM, again, enormously difficult. An uneven contour for the cold-rolled palladium never amounted to more than a few nanometres from high point to low point, whereas that for the palladium cathode usually yielded micrometre variations along the z scale.

An intriguing set of information gathered by the AFM is the tight vertical-scale force-mode images of Figs. 9a through 9d. Figure 9a displays a slightly knotted surface of the cold-rolled palladium chip, the roughest portion that was found for either side of this sample. Figure 9b displays a pattern on the concave side of the palladium cathode not seen before. There appear to be solid "puddles" distributed in this particular area. Figures 9c and 9d are magnified scans of the same area, illustrating the existence of two surface features here: a faceted particle and an irregular amorphous structure intermingled with nodules. Height-mode images indicate that the large, blocky formation of Fig. 9c rises >1 μm above the rest of the surface. These same structures appear to be coated with a heavy, "liquidlike" overlay, indicating that parts of

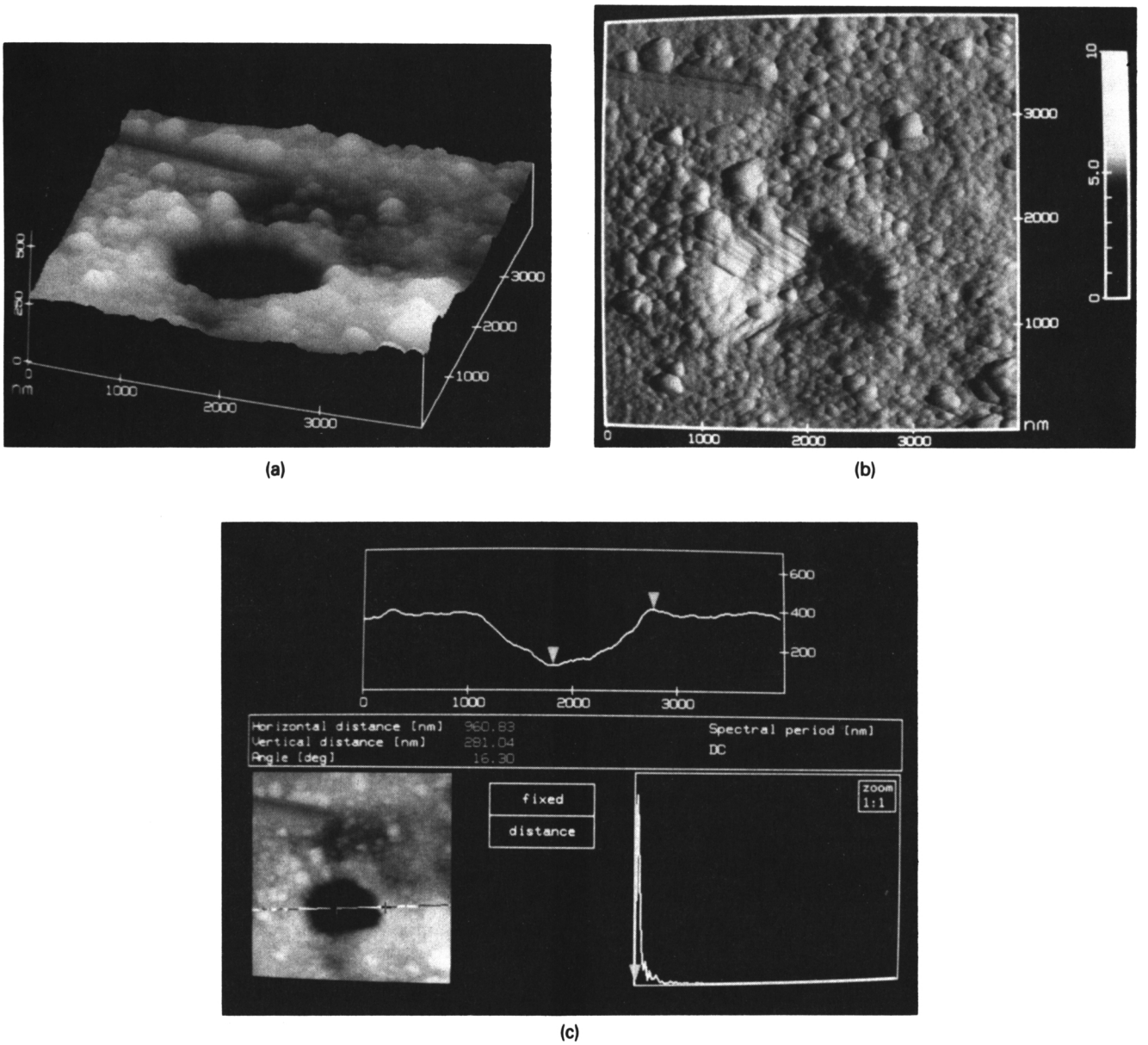

Fig. 5. A bowl-shaped cavity in palladium cathode, illustrated (a) in the height mode and (b) in the force mode, showing striations that converge into its center, and (c) contour of the crater. The crater drops >280 nm vertically from its rim.

their structures gradually flow outward from their bases into the nodules.

DISCUSSION OF RESULTS

These results document the microscopic changes in the surface morphology of a palladium cathode after electrolysis for 12 min in an electrolyte containing appreciable amounts of hydrogen ions along with deuterium ions. The surface craters observed with the SEM, and especially the AFM, have characteristics of crystal-like faceted features that make up much of their interiors, which could suggest that localized melting occurred there. The height-mode images and depth profiles showing rims around the craters suggest the possibility that molten material was ejected and solidified around the craters. Other surface features, such as the existence of mountain structures, flow structure, and variations in planar elevations, none of which was seen on the cold-rolled palladium chip, suggest that morphological changes had indeed occurred. The surface damage could be caused by chemical interaction with the electrolyte or mechanical damage caused by the formation of palladium hydride or deuteride. Chemical interaction is ruled out by the observation that palladium is chemically inert in the electrolyte (Fig. 1). The formation of rimmed craters with faceted crystals inside seems incompatible with either chemical or electrochemical processes. Surface rupture might result from swelling caused by hydride or deuteride formation, but linear cracking, rather than cratering, would be the likely result. For example, a pattern of surface cracks occurs when chromium hydride forms during

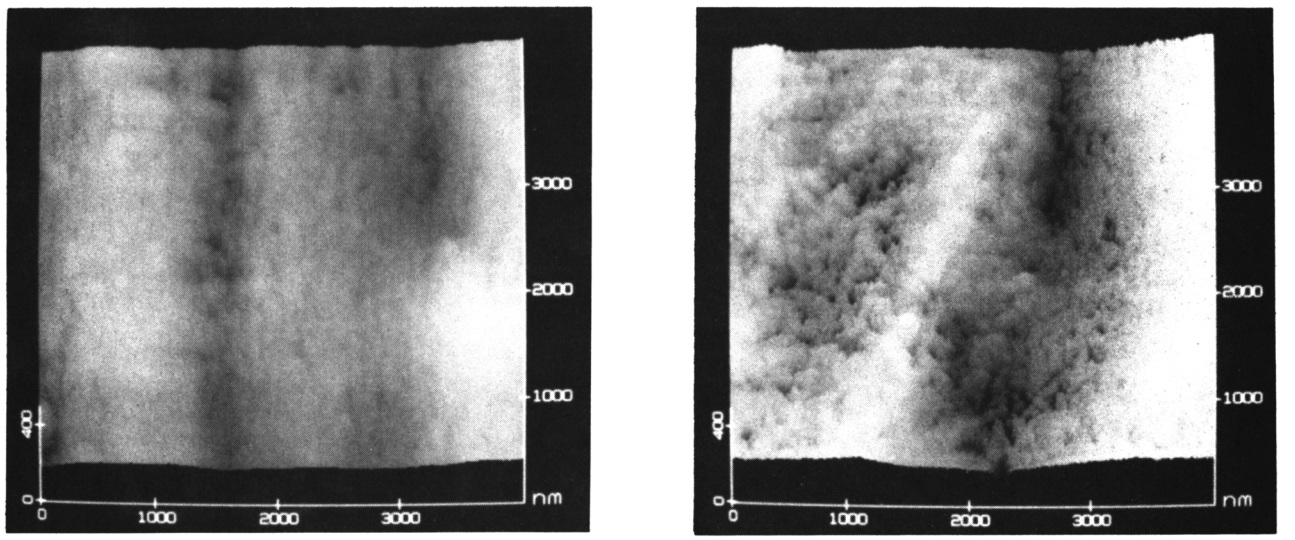

Fig. 6. STM images of (a) cold-rolled palladium foil and (b) electrolyzed palladium cathode. With the same z scale for both images (left axis) as well as a similar light intensity and contrast for photographic purposes, (b) demonstrates greater porosity and surface roughness.

electroplating of chromium.[5] The surface of electroplated chromium has a nodular appearance, but there is no evidence of surface craters.

Figure 2 shows that the lines from cold rolling are not apparent on the concave side of the cathode, which faced the anode during electrolysis. The irregular lines on Fig. 2b resemble features that form during thermal etching of a metal at elevated temperatures. Figure 9 shows amorphous features that might arise from rapid cooling of a liquid metal.

Studies by STM have been performed *ex situ* on the surface of a palladium cathode after electrolysis in aqueous H_2SO_4 (1.5 mol·dm^{-3}) for 3 h with constant cathodic current density of 500 mA/cm^2 (Ref. 4). The surface changed from smooth to nodular, but there was no evidence for cratering. The dimensions of the palladium cathode used in this study were not stated.

When a control cell with electrolyte containing light water and sulfuric acid is electrolyzed in series with the heavy water cell, the macroscopic distortion of the thin-foil palladium cathodes is of the same type in the two cells but much less in the light water cell than in the heavy water cell. Along with the greater distortion, the temperature of the heavy water cell increases more than that of the light water cell. These effects are quite reproducible.[6,7] Thus, a heavy water cell with a palladium cathode reproducibly undergoes more macroscopic distortion and generates more heat than an identical

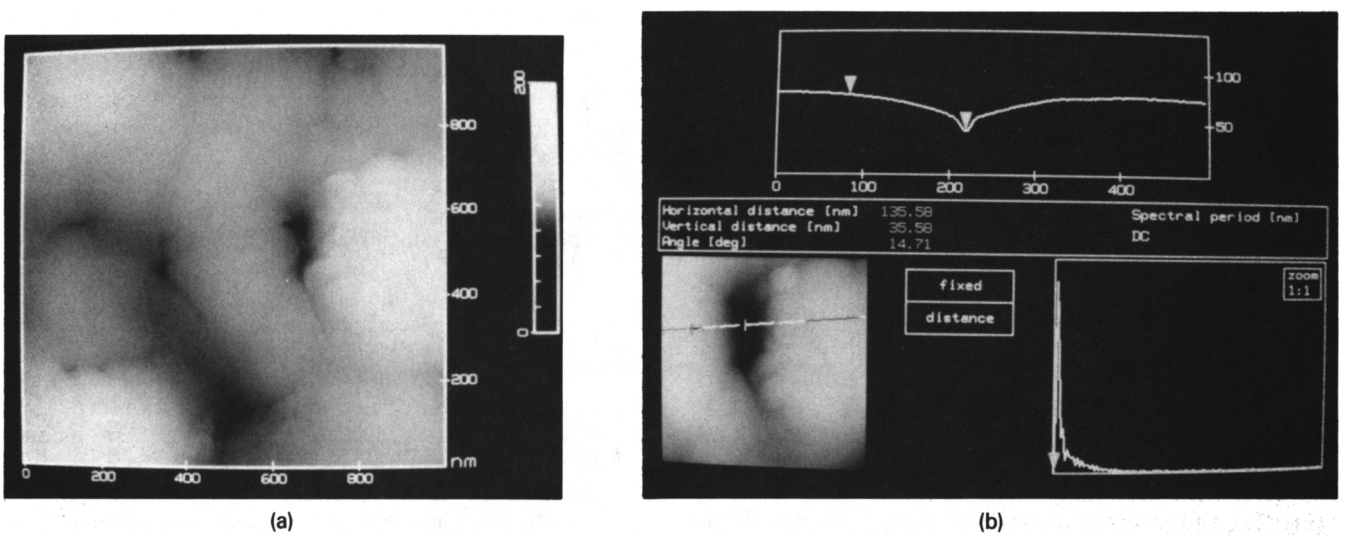

Fig. 7. (a) STM image of electrolyzed palladium cathode, showing microscopic pits and (b) profile of one of the pits.

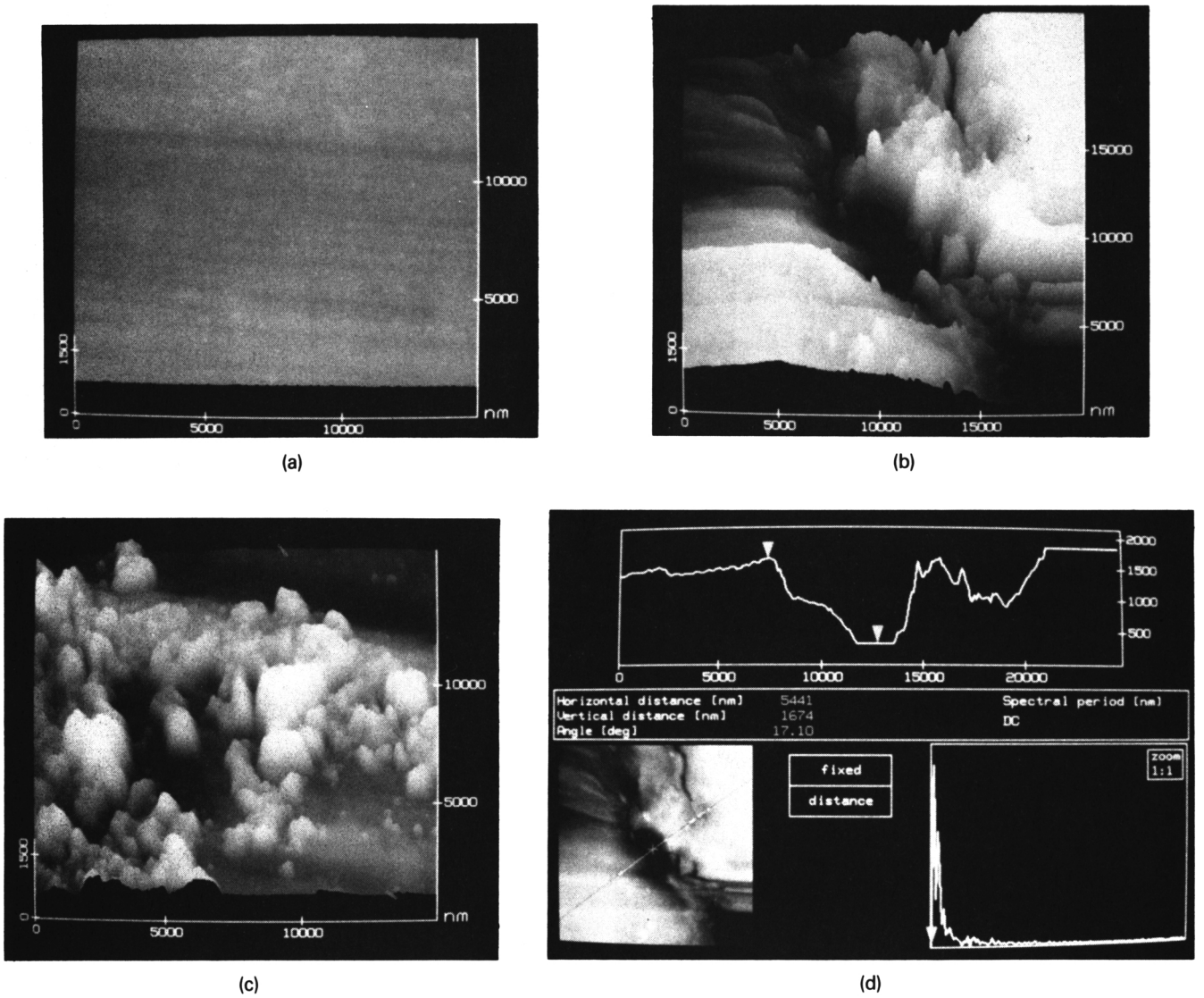

Fig. 8. AFM images of (a) cold-rolled palladium surface in the height mode and (b) concave side of palladium cathode surface in the height mode, showing steep cratering (surface levels vary in height); (c) another area revealing a mountainous region; and (d) profile of (b) illustrating surface roughness. The center pit drops >1.6 μm below the outlining area. Note that the z scale is identical for all images here.

light water cell connected in series with the same amount of power entering both cells.

CONCLUSIONS

The following conclusions can be drawn from this study:

1. Electrolysis with a thin, cold-rolled palladium cathode in an electrolyte containing both hydrogen and deuterium ions produces macroscopic deformation of the palladium. This deformation begins at the start of electrolysis, and it is quite reproducible.

2. After electrolysis for 12 min, a palladium cathode contained microscopic craters. One of these craters has microscopic needles extending from the surface into the crater (Fig. 2a), and others have rims protruding above the surface (Figs. 4, 5, and 8). Faceted crystals occur inside some of these craters (Figs. 3 and 5). The morphology of these features suggests that localized high internal temperature and pressure occurred during electrolysis and that this resulted in microscopic surface eruptions.

3. The reaction that produced localized high temperature and pressure sufficient to cause cratering is not known. Attempts to detect possible fusion by-products such as tritium and gamma and neutron radiation were not successful. However, we recently reported localized concentrations of elements that may have resulted from transmutations caused by neutrons from fusion reactions.[8,9]

ACKNOWLEDGMENTS

D. Howard kindly provided the palladium single crystal we used. We are grateful to Phillips Laboratory, Fundamental Technologies Division, at Edwards Air Force Base, for permission to use the AFM and STM for this research.

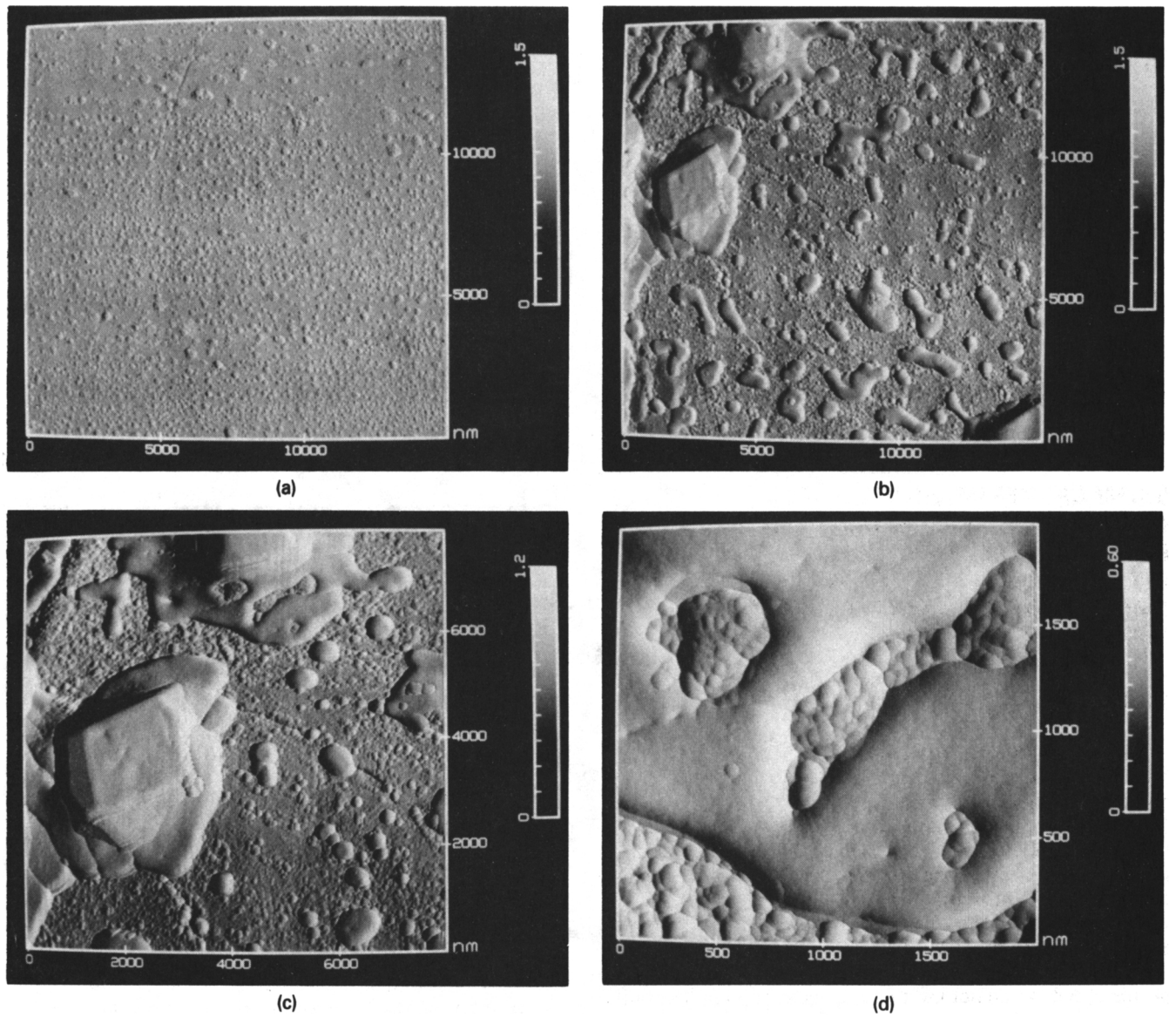

Fig. 9. Force-mode images of (a) cold-rolled palladium surface, showing a uniformly flat area with small nodules; (b) an unusual feature on the concave side of the electrolyzed palladium; (c) an enlargement of (b) concentrating on a smooth, polyhedral structure; and (d) a 2-μm scan revealing a smooth surface area interfacing with one of nodular structure.

REFERENCES

1. M. FLEISCHMANN, S. PONS, and M. HAWKINS, "Electrochemically Induced Nuclear Fusion of Deuterium," *J. Electroanal. Chem.*, **261**, 301 (1989); see also Erratum, *J. Electroanal. Chem.*, **263**, 187 (1989).

2. S. E. JONES et al., "Observation of Cold Nuclear Fusion in Condensed Matter," *Nature*, **338**, 737 (1989).

3. J. SCHWINGER, "Cold Fusion: A Hypothesis," *Z. Naturforsch*, **45a**, 756 (1990).

4. T. OHMORI, K. SAKAMAKI, K. HASHIMOTO, and A. FUJISHIMA, "Observation of Electrochemically Hydrogenated Palladium Using a Scanning Tunneling Microscope," *Chem. Lett. (Jpn)*, 93 (1991).

5. A. M. KASAAIAN and J. DASH, "Effect of Methanol and Formic Acid on Chromium Plating," *Plating Surf. Finishing*, **71**, *11*, 66 (1984).

6. P. S. KEEFE, "Comparison of Light and Heavy Water Electrolysis with Palladium Cathodes," MS Thesis, Portland State University (1990).

7. J. DASH, P. S. KEEFE, E. NICHOLAS, and D. S. SILVER, "Comparison of Light and Heavy Water Electrolysis with Palladium Cathodes," *Proc. 80th Ann. Conf. American Electroplaters and Surface Finishers Society*, Orlando, Florida, June 1993, p. 755.

8. J. DASH and G. NOBLE, "Surface Morphology and Microcomposition of Palladium Cathodes After Electrolysis in Acidified Light and Heavy Water," submitted to 4th Int. Conf. Cold Fusion, Lahaina, Hawaii, December 6-9, 1993.

9. J. DASH and D. DIMAN, "Localized Melting and Microcomposition of a Pd Cathode After Electrolysis in Acidified Heavy Water," submitted to 4th Int. Conf. Cold Fusion, Lahaina, Hawaii, December 6-9, 1993.